Hindawi
Journal of Chemistry
Volume 2019, Article ID 4360175, 12 pages
https://doi.org/10.1155/2019/4360175

Research Article

Isoflavones and Isoflavone Glycosides: Structural-Electronic Properties and Antioxidant Relations—A Case of DFT Study

Son Ninh The,[1] **Thanh Do Minh**,[2] **and Trang Nguyen Van**[2]

[1]*Institute of Natural Products Chemistry, Vietnam Academy of Science and Technology (VAST), 18 Hoang Quoc Viet, Caugiay, Hanoi, Vietnam*
[2]*Institute for Tropical Technology, Vietnam Academy of Science and Technology (VAST), 18 Hoang Quoc Viet, Caugiay, Hanoi, Vietnam*

Correspondence should be addressed to Son Ninh The; yamantson@gmail.com and Trang Nguyen Van; nguyenvantrangsphn1909@gmail.com

Received 8 January 2019; Revised 13 February 2019; Accepted 24 February 2019; Published 24 June 2019

Academic Editor: Artur M. S. Silva

Isoflavonoids and isoflavonoid glycosides have drawn much attention because of their antioxidant radical-scavenging capacity. Based on computational methods, we now present the antioxidant potential results of genistein (**1**), biochanin A (**2**), ambocin (**3**), and tectorigenin 7-*O*-[*β*-D-apiofuranosyl-(1-6)-*β*-D-glucopyranoside] (**4**). The optimized structures of the neutral and radical forms have been determined by the DFT-B3LYP method with the 6-311G(d) basis set. From the findings and thermodynamic point of view, the ring B system of isoflavones is considered as an active center in facilitating antioxidant reactions. Antioxidant activities are mostly driven by O-H bond dissociation enthalpy (BDE) following hydrogen atom transfer (HAT) mechanism. Antioxidant ability can be arranged in the following order: compounds (**4**) > (**3**) > (**2**) > (**1**). Of comprehensive structural analysis, flavonoids with 4′-methylation and 6-methoxylation, especially 7-glycosylation would claim responsibility for antioxidant enhancement.

1. Introduction

Naturally occurring isoflavone compounds fall into the class of flavonoid phenolic compounds, which consists of a molecular structure of 3-phenylchromen-4-one backbone, and are widely distributed in the plant kingdom, particularly in Fabaceae family [1]. Isoflavone derivatives were found to involve in various biological experiments and have been employed in pharmacological drugs to treat cancer, Alzheimer's disease, atherosclerosis, and so on [2]. Basically, the reactive oxygen radicals such as hydroxyls (˙OH) presenting in living organisms can be seen as the reason for the changes in the body and one of the main causes of various diseases [3]. Numerous evidence suggests that either flavonoids or typical isoflavones have been shown to be associated with good antioxidant capacities due to their radical-scavenging activities.

Of computational compounds **1–4**, we herein select the best isoflavones and their 7-glycosylation principally based on the good results in their biological experiments, including genistein (**1**), biochanin A (**2**), ambocin (**3**), and tectorigenin 7-*O*-[*β*-D-apiofuranosyl-(1-6)-*β*-D-glucopyranoside] (**4**) (Figure 1) [4, 5]. A vast data showed that the substitutions at C-5, C-7, and C-4′ in isoflavonoid rings have been playing a key role in structural features of bioactive isoflavones, especially in terms of antioxidants [4]. For instance, genistein (**1**) revealed much more significance in the powerful antioxidant when compared to other isoflavones like daidzein and glycitein due to the dependence on its functional hydroxyl groups [5]. Likewise, a survey conducted by Dowling et al. proposed that with regards to DPPH (2,2-diphenyl-1-picrylhydrazyl) assay, both genstein (**1**) and its 4′-methoxylation biochanin A (**2**) successfully chelated to Cu (II) and Fe (III) with a 1 : 2 M/L stoichiometry in methanol phase, whereas daidzein fails to do so [6].

Using B3LYP functional with 6-311G(d) basis set for studied mediums gas and methanol, the current DFT (density functional theory) study will provide an insight into structural features, conformational analyses, and electronic properties of the selective isoflavones **1**-**2**, in which the result intensively related to explaining their reactivity with free radicals. Ambocin (**3**) was isolated from the root of *Pueraria*

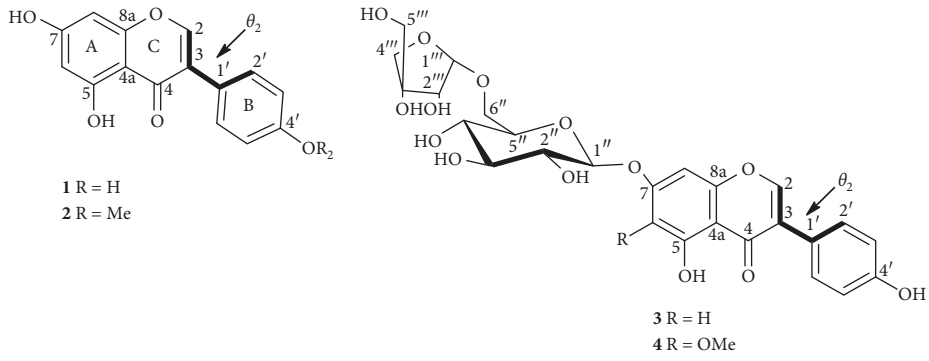

(a) (b)

Figure 1: General structures of studied compounds **1–4** with atom numbering.

mirifica, while its 6-methoxylation compound (**4**) had recently been identified as a new compound existing in *Dalbergia sissoo* stem bark [4, 7]. To the best of our knowledge, there have been no specific theoretically useful account reports on their glycosides **3-4**. Therefore, we also set out a computational work on 7-glycosylated compound (**3**) and 6-methoxylated-7-glycosylated compound (**4**), within the aim of finding the effects of chemical structure on the antioxidant capacity. Hopefully, the findings will lay the ground for future research.

1.1. Theoretical Parameters and Computational Procedure. DFT calculation is carried out with Gaussian 09 software package [8]. In order to optimize the structure, the B3LYP exchange correlation functional level without constraints has been utilized and has been linked to 6-311G(d) basis set in the gas phase (dielectric constant, $\varepsilon = 1$) and in methanol solvent ($\varepsilon = 32.613$) [9, 10]. Vibrational frequencies are calculated at the same level to correct zero-point energy (ZPE). The result confirms the presence of ground states without imaginary frequency. The self-consistent reaction field polarizable continuum model (SCRF-PCM) has been employed for estimating solvent effects [9].

From literature, there have been three known mechanisms HAT (H-atom Transfer), SET-PT (Single electron transfer-proton transfer), and SPLET (Sequential proton loss electron transfer), which concern radical-scavenging properties of the parent molecular (Flav-OH) [11–17]:

(1) HAT mechanical route (Equation (1)) involves in O-H bond breaking of Flav-OH, then transfers to radicals, and is often controlled by homolytic bond dissociation enthalpy (BDE) (Equation (2)).

$$\text{Flav-OH} + \text{RO}^{\bullet} \longrightarrow \text{Flav-O}^{\bullet} + \text{ROH} \tag{1}$$

$$\text{BDE} = \text{H}\left(\text{Flav-O}^{\bullet}\right) + \text{H}\left(\text{H}^{\bullet}\right) - \text{H}\left(\text{Flav-OH}\right) \tag{2}$$

H(Flav-O$^{\bullet}$), H(H$^{\bullet}$), and H(Flav-OH) are the enthalpies of Flav-O$^{\bullet}$, hydrogen radical atom, and the parent flavonoid molecule, respectively.

(2) SET-PT pathway was recognized by two steps (Equation (3)). In details, the first step accounted for the process of losing an electron to form molecular radical cation Flav-OH$^{\bullet+}$. After that, Flav-OH$^{\bullet+}$ was deprotonated. The first action was evaluated by the sum of the ionization potential (IP), whereas deprotonation was characterized by heterolytic bond dissociation enthalpy (PDE) (Equations (4) and (5)).

$$\begin{aligned}\text{Flav-OH} + \text{R}^{\bullet} &\longrightarrow \text{Flav-OH}^{\bullet+} + \text{R}^{-} \\ &\longrightarrow \text{Flav-O}^{\bullet} + \text{ROH}\end{aligned} \tag{3}$$

$$\text{IP} = \text{H}\left(\text{Flav-OH}^{\bullet+}\right) + \text{H}\left(\text{e}^{-}\right) - \text{H}\left(\text{Flav-OH}\right) \tag{4}$$

$$\text{PDE} = \text{H}\left(\text{Flav-O}^{\bullet}\right) + \text{H}\left(\text{H}^{+}\right) - \text{H}\left(\text{Flav-OH}^{\bullet+}\right) \tag{5}$$

H(Flav-OH$^{\bullet+}$) presents the enthalpies of flavonoid radical cation Flav-OH$^{\bullet+}$ after electron abstraction of original flavonoid. The calculated gaseous phase enthalpy values, which are 0.75 kcal/mol and 1.48 kcal/mol, are normally used for H(e^{-}) and H(H^{+}), respectively [11, 12].

(3) The third mechanical SPLET is briefly described when flavonoid is deprotonated to afford a typical anion Flav-O^{-} and the sequential electron transfer from this anion happens (Equation (6)). Proton affinity (PA) and the electron transfer enthalpy (ETE) are two conceptual parameters which correspond to deprotonation and electron transfer, respectively (Equations (7) and (8)).

$$\begin{aligned}\text{Flav-OH} &\longrightarrow \text{Flav-O}^{-} + \text{H}^{+}; \text{Flav-O}^{-} + \text{R}^{\bullet} \\ &\longrightarrow \text{Flav-O}^{\bullet} + \text{R}^{-}; \text{R}^{-} + \text{H}^{+} \longrightarrow \text{RH}\end{aligned} \tag{6}$$

$$\text{PA} = \text{H}\left(\text{Flav-O}^{-}\right) + \text{H}\left(\text{H}^{+}\right) - \text{H}\left(\text{Flav-OH}\right) \tag{7}$$

$$\mathrm{ETE} = \mathrm{H}\left(\text{Flav-O}^{\bullet}\right) + \mathrm{H}\left(\mathrm{e}^{-}\right) - \mathrm{H}\left(\text{Flav-O}^{-}\right) \quad (8)$$

H(Flav-O$^-$) is the enthalpy of flavonoid anion after proton abstraction of original molecule.

Antioxidant activities have been explained by DFT-based reactivity descriptors [11], including energies of highest occupied molecular orbital (HOMO) and lowest unoccupied molecular orbital (LUMO), dipole moments, atomic charges, electron affinity A, the ionization potential I_o, the global hardness η, the electronegativity χ, the chemical potential μ, global electrophilicity index ω, and Fukui chemical parameters.

Based on the theoretical approach of DFT, Janak's theorem, and the finite difference approximation, these descriptors can be proposed by the related equations given as follows [18]:

$$\begin{aligned} I_o &\approx -E_H, \\ A &\approx -E_L, \\ \eta &\approx \frac{(I_o - A)}{2} \approx \frac{(E_L - E_H)}{2}, \\ \chi &\approx \frac{(I_o + A)}{2} \approx \frac{(E_L + E_H)}{2}, \\ \mu &\approx -\frac{(I_o + A)}{2} \approx \frac{-(E_L + E_H)}{2}, \end{aligned} \quad (9)$$

where E_H and E_L are energies of HOMO and LUMO, respectively.

The atomic charges for neutral molecular were restricted by Mulliken population analysis (MPA) following the same framework of B3LYP/6-311G(d).

The global electrophilicity index ω indicates the stabilization energy of a molecule system when being saturated by electrons from outside. Therefore, the higher value of ω^+ (electron accepting) shows the significant electrophilicity while the lower one of ω^- (electron donating) evidently exhibits the better nucleophilicity of a compound. These chemical indices were expressed following the functions as follows [19]:

$$\begin{aligned} \omega &= \frac{\mu^2}{2\eta} \approx \frac{(I_o + A)^2}{[4(I_o - A)]} \approx \frac{(E_L + E_H)^2}{[4(E_L - E_H)]}, \\ \omega^- &= \frac{(3I_o + A)^2}{[16(I_o - A)]}, \\ \omega^+ &= \frac{(I_o + 3A)^2}{[16(I_o - A)]}. \end{aligned} \quad (10)$$

As a general conceptual comprehension, the condensed Fukui parameters evidently provide information on a selective property in a chemical reaction. The atom coupled with the high electronic population displays as the most reactive site when compared to the surrounding atoms in a molecule [20]. Briefly, Fukui descriptors have been shown to associate with nucleophilic (f_k^+), electrophilic (f_k^-), and/or radical attacks (f_k^0) and were possibly described by the following equilibriums [20]:

$$\begin{aligned} f_k^+ &= q_k(N+1) - q_k(N), \\ f_k^- &= q_k(N) - q_k(N-1), \\ f_k^0 &= \frac{[q_k(N+1) - q_k(N-1)]}{2}, \end{aligned} \quad (11)$$

where $q_k(N)$: electronic population of atom k in a neutral molecule, $q_k(N+1)$: electronic population of atom k in an anionic molecule, and $q_k(N-1)$: electronic population of atom k in a cationic molecule.

2. Results and Discussion

2.1. Geometrical Analysis. The comprehension of isoflavone conformational analysis is an important method to prove the relationship between the antioxidant activities and structural aspects since the HAT, SET-PT, and SPLET pathways closely depend on the behaviors of differential hydroxyl groups and the geometric features. From Figures 2 and S1 and Table 1, we reported the optimized structures with patterns of intramolecular hydrogen bonds (IHBs) between 5-OH and 4-CO, along with selective characters of bonds, bond angles, and dihedral angles. As of local minimum energies, there is no distinction in each compound between gaseous state and methanol (Table 2). The first feature observed from the optimized molecular structures of **1–4** is that π-electron is delocalized in the whole aglycone, especially B towards C through 2,3-double, and the coplanar between chromene ring and phenyl unit is lost. In agreement with findings of IHBs in many previous flavonoid DFT calculated researches [21], IHBs lengths are found to be 1.721 Å for **1**-**2**, 1.726 Å for **3**, and 1.733 Å for **4** in gas. When compared to 5-OH and 7-OH, the longer bond lengths of 4′-OH and O-C_1'' at 7-position evidently reinforces that, as a matter of fact, hydrolysis reactions occurred in flavone glycosides at aglycone-glycone linkage, or antioxidant activations facilitated at 4′-OH for flavonoids [22, 23]. As shown in Table 1, bond angles θ_1 (4′-O-H) and θ_1 (7-O-H) demonstrate larger 2-3° than θ_1 (5-O-H), obviously caused by effective IHBs.

Regarding the effects of environmental researches, especially polar solvents, we now select methanol as a good agent because it promotes many biological processes [24]. So far, flavonoids are recognized as weak polar compounds and that it is not easy to dilute them in water [25]. In comparison with gaseous circumstance, methanol directly induces the reduction of IHBs lengths and the elongation of 5-OH bond lengths. Also, 6-OCH_3 can be seen as the main reason that makes a slight difference in IHBs between compounds **3** and **4** in the procedures of both gas and methanol. Dihedral angles θ_1 (C_2-C_3-$C_{1'}$-$C_{2'}$) among all structures **1–4** show not much change and reach 41.5° in gas and 44° in methanol. From previous literature data, utilizing the RHF/6-311 + G(d) *ab initio* method, compounds **1**-**2** have been linked to θ_1 numbers of 40° and 45° in environmental acetonitrile or regarding to employment of UB3LYP/6-

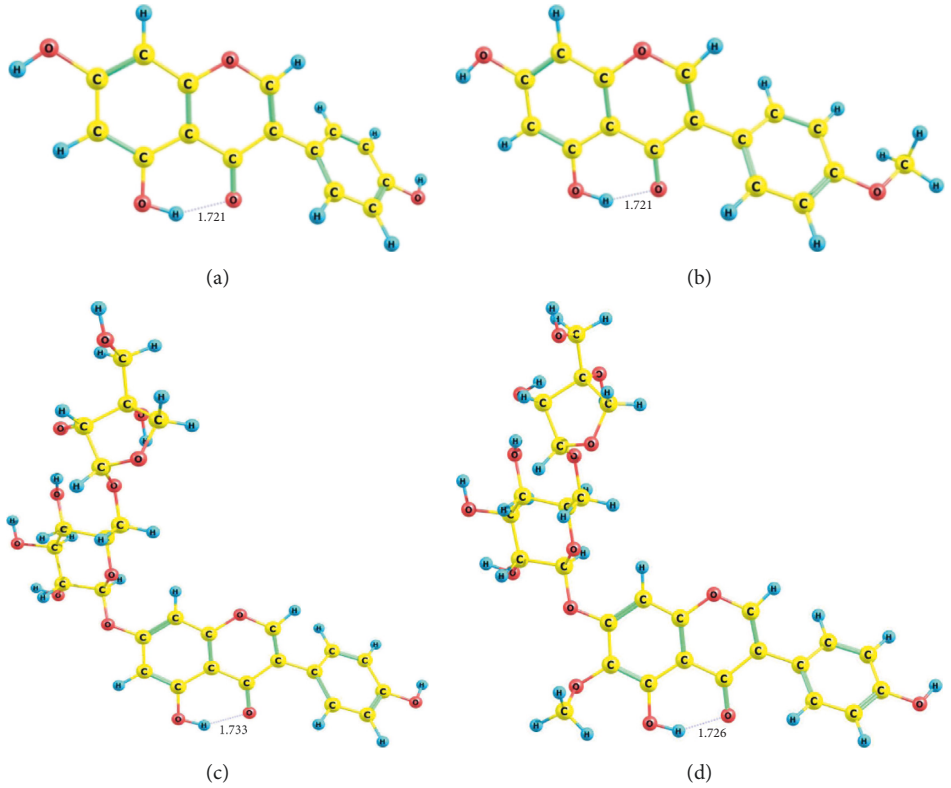

Figure 2: State forms of studied structures **1–4** in gas medium. (a) Compound **1**. (b) Compound **2**. (c) Compound **3**. (d) Compound **4**.

Table 1: Optimized bond distances, bond angles (θ_1), and dihedral angles (θ_2) of studied compounds with B3LYP/6-311G(d) in gas and methanol mediums.

	No.	Bond lengths						
		5 (O-H)	7 (O-H)	7 (O-C1″)	6 (O-CH_3)	4′ (O-H)	4′ (O-CH_3)	Hydrogen bonds
1	Gas	1.337	1.357			1.364		1.721
	Methanol	1.343	1.354			1.364		1.714
2	Gas	1.337	1.357				1.362	1.721
	Methanol	1.343	1.354				1.361	1.714
3	Gas	1.338		1.365		1.365		1.733
	Methanol	1.343		1.365		1.364		1.720
4	Gas	1.338		1.365	1.364	1.365		1.726
	Methanol	1.343		1.362	1.370	1.364		1.716

	No.	Bond angles				Dihedral angles
		θ_1 (C_5-O-H)	θ_1 (C_7-O-H)	θ_1 ($C_{4'}$-O-H)	θ_1 (C_2-C_3-$C_{1'}$)	θ_2 (C_2-C_3-$C_{1'}$-$C_{2'}$)
1	Gas	107.450	109.900	109.748	120.378	41.491
	Methanol	107.122	110.640	110.240	120.286	44.364
2	Gas	107.459	109.886		120.342	41.492
	Methanol	107.106	110.620		120.273	44.440
3	Gas	107.631		109.726	120.316	41.531
	Methanol	107.791		110.207	120.214	43.576
4	Gas	107.631		109.726	120.642	41.531
	Methanol	106.792		110.241	120.189	44.128

31++G (d,p) in gas phase and θ_1 value of 39.3° was recorded for genistein (**1**) [22, 26], but no manuscript associates with an insight into relationships between conformations and their energies.

To confirm the results mentioned above, potential energy curves for all considered compounds **1–4** are obtained, like the functions of torsional angle θ_2 (C_2-C_3-$C_{1'}$-$C_{2'}$) between the rings B and C linkage in the gaseous state. In this case, θ_2 has been explored by scanning in the characteristic steps of 15° values from 0° to 360° at theoretical level B3LYP/6-311G(d) (Table S1). An attempt to accurate, without any constraints, the structures of these four isoflavones is then optimized around each conformational potential minimum, and the results are drawn in Figure 3. It can generally be

Table 2: Chemical reactivity indices obtained using the DFT method in gas and methanol mediums.

No.	Medium	η (eV)	χ (eV)	μ (eV)	I_o (eV)	A (eV)	ω (eV)		
							ω	ω^-	ω^+
1	Gas	2.125	3.835	−3.835	5.960	1.710	3.461	5.644	1.809
	Methanol	2.124	3.932	−3.932	6.056	1.808	3.639	5.871	1.939
2	Gas	2.107	3.789	−3.789	5.897	1.682	3.407	5.565	1.776
	Methanol	2.109	3.915	−3.915	6.024	1.806	3.633	5.854	1.940
3	Gas	2.134	3.758	−3.758	5.891	1.624	3.309	5.455	1.697
	Methanol	2.115	3.967	−3.967	6.081	1.852	3.720	5.968	2.001
4	Gas	2.086	3.710	−3.710	5.796	1.624	3.299	5.415	1.705
	Methanol	2.093	3.956	−3.956	6.049	1.863	3.740	5.979	2.023

No.	Medium	Dipole moment (debye)	Polarizability (au)	Energy (kcal/mol)	E_{HOMO} (eV)	E_{LUMO} (eV)
1	Gas	3.036	187.118104	−598608.14	−5.960	−1.710
	Methanol	4.455	247.343170	−598618.59	−6.056	−1.808
2	Gas	2.862	202.392352	−623276.98	−5.897	−1.682
	Methanol	4.231	264.841735	−623285.97	−6.024	−1.806
3	Gas	10.227	347.615084	−1293394.88	−5.891	−1.624
	Methanol	13.200	440.126098	−1293415.13	−6.081	−1.852
4	Gas	10.069	365.799666	−1365267.47	−5.796	−1.624
	Methanol	13.537	461.553236	−1365289.45	−6.049	−1.863

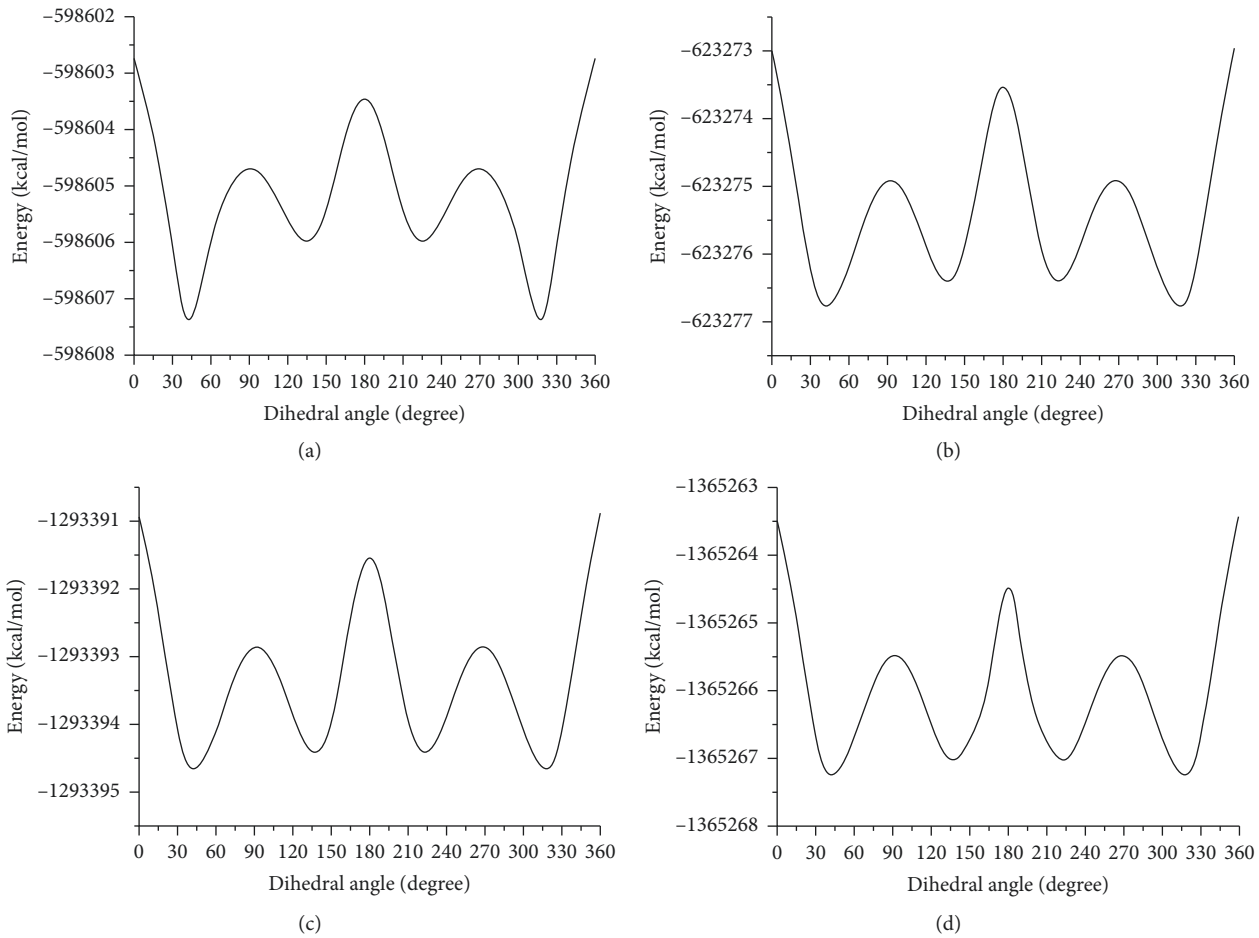

Figure 3: Potential energy curves versus torsional angle of studied structures **1–4** in gas medium. (a) Compound **1**. (b) Compound **2**. (c) Compound **3**. (d) Compound **4**.

noted that the dependence of conformational states on torsional angle θ_2 is similar among all isoflavonoids **1–4**, including two conformers I-II lying at 41.5° (conformer I) and 135° (conformer II) for each molecule. These two conformers arise from the potential energy versus torsional angles obtained as a good agreement with the previous

publication on several isoflavones [11]. The absolute minimum I is more stable than the conformational relative minimum II by 1.98 kcal/mol for genistein (**1**); however, this one for compounds **2–4** has smaller values of 0.40 kcal/mol, 0.29 kcal/mol, and 0.26 kcal/mol, respectively. Parallel with this, there are several potential energy barriers that range from I to II in compound **1**; the first interconversion energy barrier's value of 3.55 kcal/mol is recognized at the perpendicular conformation ($\theta_2 = 90^\circ$), and the second energy barrier accounts for 4.94 kcal/mol and peaks at *anti* ($\theta_2 = 180^\circ$) conformation; meanwhile, the maximum interchangeable barrier reaches 5.41 kcal/mol at *syn* ($\theta_2 = 360^\circ$ or 0°) shape. In the same manner, with torsional angles θ_1 of 90°, 180°, and 360° (or 0°), these potential energy barriers are found at the values of 2.15 kcal/mol, 3.78 kcal/mol, and 4.02 kcal/mol; 2.15 kcal/mol, 3.77 kcal/mol, and 4.00 kcal/mol; and 2.11 kcal/mol, 3.81 kcal/mol, and 4.03 kcal/mol for compounds **2–4**, respectively. The dramatic difference obtained from energies between two minima, together with the distinction from the interchangeable energy barriers of **1** and groups **2–4** can be explained by the symmetric property of **1**, the phenomena of 4′-methylation in **2**, 7-glycosylation in **3**, and 6-methoxylation-7-glycosylation in **4**.

2.2. Frontier Molecular Orbital Theory and Spin Density. Taking π-electron delocalization into consideration, it involves in the stabilization of parent molecular and radicals after H abstractions [27]. The frontier orbital theoretical calculation seems to be a significant tool for explaining the relationship between neutral and radical forms, especially in terms of the electron delocalization. At the level of B3LYP/6-311G(d) in both mediums of gas and methanol, HOMO and LUMO of neutral and radical visual images and frontier orbital energies of **1–4** are shown in Figures 4–6 and Table 2. HOMO neutral images show that the electron distribution is concentrated in the entire aglycone, especially ring B and 2,3-double bond, while LUMO neutral is delocalized over systematic rings A and C. Sugar units are not a suitable site for radical reactions. The same result has been found in previously studied isoflavones glycitein, pratensein, and prunetin [11]. When hydrogen atom abstraction takes place in four isoflavones, it is worth noting that 4′-OH HOMO radical species in compounds **1** and **3-4**, which correspond to the small BDE values, consist of high electron density in ring B and slightly less in ring A. 5-OH, and/or 7-OH HOMO radical shapes, which concern the high BDE values, did not differ from neutral composition except for the less electron distribution in ring C for 5-OH radical site of compound **4**. LUMO radical forms mostly focus on chromene systems but slightly view in ring B in the case of 5-OH, 7-OH of compounds **1-2**, and 5-OH of compounds **3-4**. The higher E_{HOMO} (the lower ionization potential I_o), and the lower E_{LUMO} (the higher electron affinity A) mean the better capacity of electrons donating and the better sensitivity to receive electrons, respectively, whereas the easier electron transfer indicates the lower $E_{gap} = E_{LUMO} - E_{HOMO}$, and thus, the better antioxidant reactivity. From Table 2, the gaseous phase would lay a better ground for decreasing

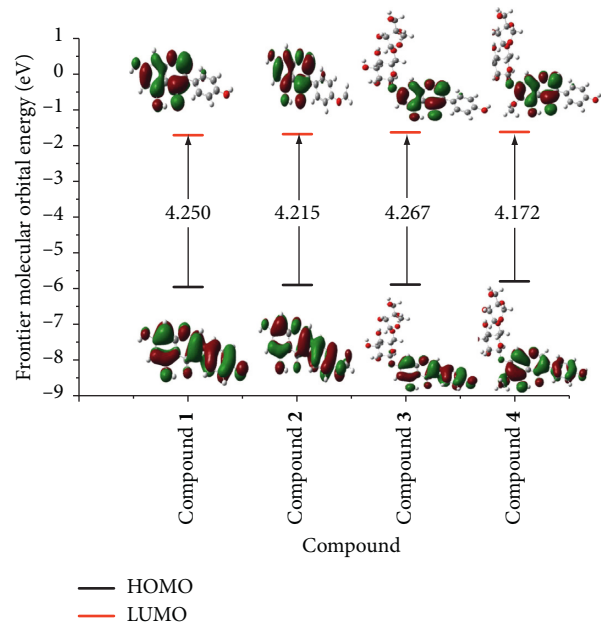

Figure 4: Neutral HOMO and LUMO images and E_{gap} of structures **1–4** in gas medium.

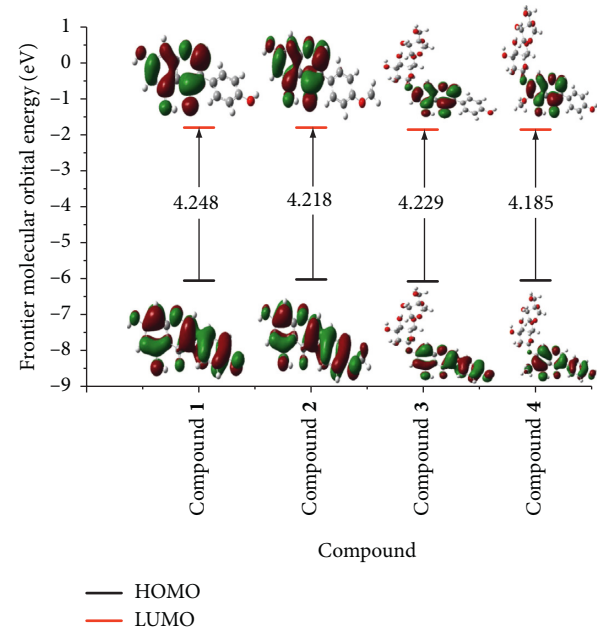

Figure 5: Neutral HOMO and LUMO images and E_{gap} of structures **1–4** in MeOH medium.

E_{HOMO} values when compared with using methanol, but methanol solution should be a suitable tool to scale down E_{LUMO} values. Paying attention to the gaseous medium, the highest E_{HOMO}, which can be claimed responsible for advantageous radical reactions, here facilitates compound **4** (−5.796 eV) in preference to the others, **3** (−5.891 eV), **2** (−5.897 eV), and **1** (−5.960 eV). The numbers of 4.250 eV, 4.215 eV, 4.267 eV, and 4.172 eV are assignable to the respective E_{gap} values of compounds **1–4** in the environmental gas. The most striking feature is that 4′-methylated

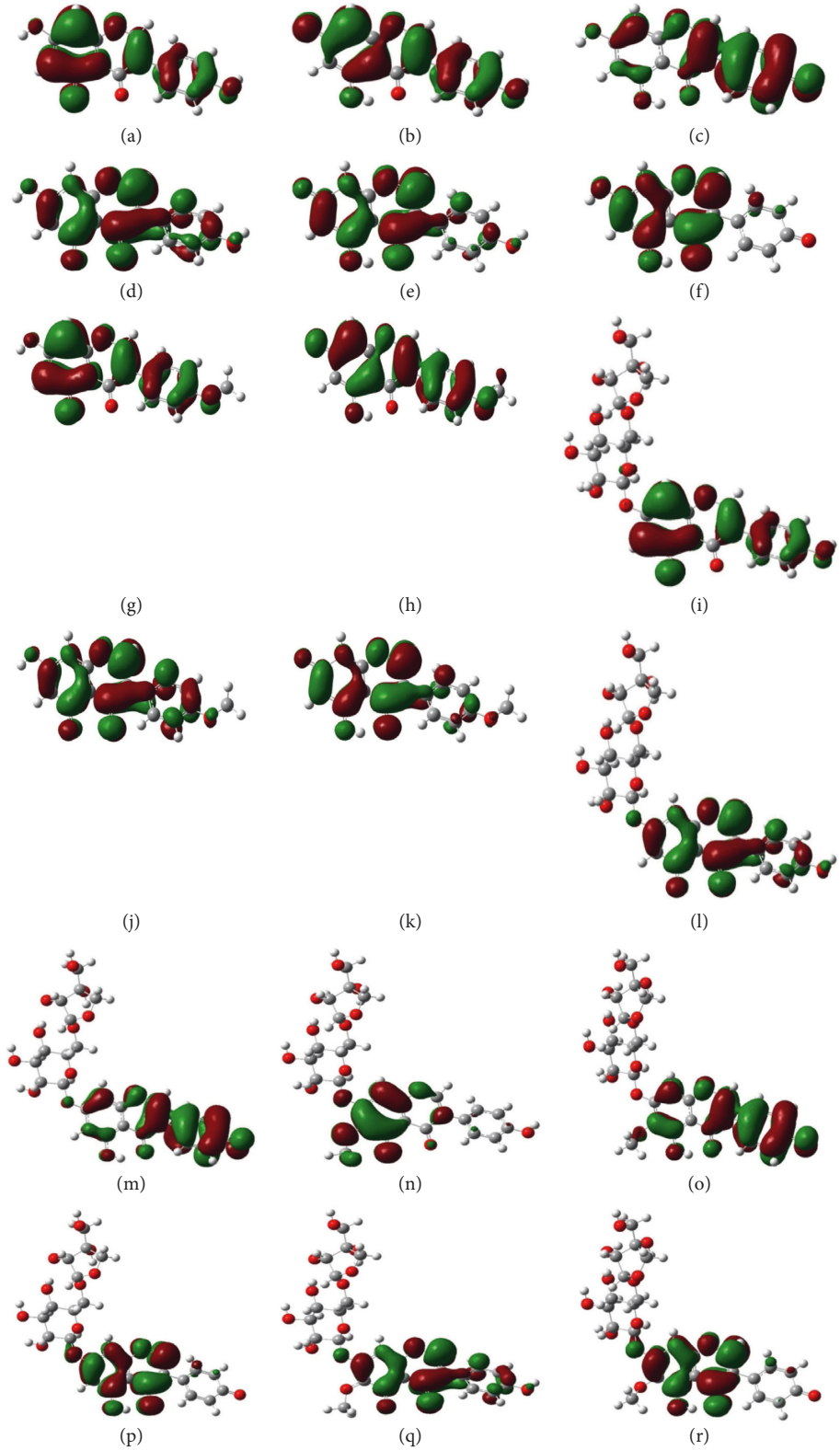

Figure 6: HOMO and LUMO of structural radicals **1–4**. (a) HOMO-5-OH radical (**1**). (b) HOMO-7-OH radical (**1**). (c) HOMO-4′-OH radical (**1**). (d) LUMO-5-OH radical (**1**). (e) LUMO-7-OH radical (**1**). (f) LUMO-4′-OH radical (**1**). (g) HOMO-5-OH radical (**2**). (h) HOMO-7-OH radical (**2**). (i) HOMO-5-OH radical (**3**). (j) LUMO-5-OH radical (**2**). (k) LUMO-7-OH radical (**2**). (l) LUMO-5-OH radical (**3**). (m) HOMO-4′-OH radical (**3**). (n) HOMO-5-OH radical (**4**). (o) HOMO-4′-OH radical (**4**). (p) LUMO-4′-OH radical (**3**). (q) LUMO-5-OH radical (**4**). (r) LUMO-4′-OH radical (**4**).

compound **2** and 6-methoxylated compound **4** evidently generate better E_{gap} values when compared to respective compounds **1** and **3** in both of the phases. Emphasizing on the change of gas phase into methanol, a remarkable reverse can be observed in the E_{gap} values between **1** and **3**, due to the 7-glycosylated phenomenon. Among four compounds **1–4**, we primarily assumed that tectorigenin 7-*O*-[*β*-D-apiofuranosyl-(1-6)-*β*-D-glucopyranoside] (**4**) is the best candidate employable for antioxidant targets, not mention the fact that 4′-methylation, 6-methoxylation, and 7-glycosylation facilitate the antioxidant ability.

Calculation of the atomic spin density population of various radicals after H-abstraction from four considered isoflavones **1–4** is given in Figure 7. It should be kept in mind that the higher the spin density delocalized in radicals, the easier the radical formation, hence lower BDE values [28]. As a general view, the computed results reveal that strong spin distributions remain on oxygen atoms of phenolic groups, carbons C-1′, C-3′, and C-5′ of the ring B, and carbons C-6 and C-8 in ring A and also C4a. In all four compounds **1–4**, C-1′, C-3′, and C-5′ are centers of positive spin density; C-2′, C-4′, and C-6′ bear negative one whilst atomic carbons in ring A fail to do so [11]. It suggests that phenyl unit ring B with more delocalized spin is significantly suitable for radical formation. The spin density values of O-atom make an order as 0.432–0.433 (7-OH in compounds **1-2**) > 0.381–0.382 (4′-OH in compounds **1**, **3-4**) > 0.310–0.376 (5-OH in compounds **1–4**). As of a normal rule, the higher spin density means higher BDE values. Nonetheless, the number of spin in O-atom is found in the opposite direction with predictable BDE values among 5-OH and 4′-OH radicals, which can be explained by the fact that H-removal needs to have suitable energy to break the hydrogen bonds between 5-OH and 4-CO [29].

2.3. Electronic Properties. The global hardness η has emerged as a measurement of resistance to charge transfer [29]. 7-Glycosylated compound (**3**) accounts for the maximum chemical hardness η value of 2.134 eV in the gaseous phase; it has been confirmed that this compound is much more stable than the remainder, particularly in comparison with the unstable 6-methoxylated-7-glycosylated compound **4** (2.086 eV in gas, 2.093 eV in methanol). By comparing compounds **1** and **2**, 4′-OCH_3 mainly causes a decrease of η in both phases. Therefore, it can be concluded that methylations and methoxylations in isoflavones and their glycosides induce a trend in transferring from "high oxidation state and low polarizability" to "low oxidation state and high polarizability."

The electronegativity χ measures a trend to attract electrons, along with the chemical potential μ which will be proportional to this parameter of a negative signal [30]. Following Sanderson's principle, a compound exerting the high electronegativity might quickly reach equalization and establish low reactivity [31]. Therefore, the low value of this one for antioxidant reactions is expected. Compound **4** with low χ value of 3.710 eV in the gaseous state participates in antioxidant reactivity better than the range of 3.758–3.835 eV for compounds **1–3**. Nevertheless, using solvents, if solvents, like medium methanol, are used, the results are greatly influenced. Indeed, it is opposite to the tendency of genistein (**1**) and biochanin A (**2**), whose glycosides **3-4** tend to go from a lower electronegativity in gas to a higher one in methanol (Table 2).

Apart from descriptors such as the electron affinity, the ionization potential, the global hardness, and the global electronegativity, the global electrophilicity index ω, ω^-, and ω^+ values have so far been increased when methanol is taken into account. The ω^- values of all considered compounds **1–4** are 2-3-folds higher than those of ω^+ in either gas or methanol method. This one is identical with the previous literature data [11], in which isoflavones and their sugar derivatives tend to donate electrons rather than capturing.

Within a molecule, the dipole moment is an available method to estimate the separation of positive and negative electrical charges. The high magnitudes of the dipole moment accompany with the high charge densities and high polarity in bonds [21]. In our current account, glycosylated compounds **3-4** is 3-folds higher than isoflavones **1-2** in both states, gas and methanol, because of the effects of sugar units and solvents. However, focusing on the comparison between **1** and **2** and **3** and **4**, 4′-methylation and 6-methoxylation are suitable for slightly reducing this property. Han and his partners pointed out that the more symmetric property in structures, the lower dipole moment, and its antioxidant efficiency is better than that of the asymmetric molecule of the same size [22]. We found that the symmetric genistein (**1**) and its 4′-methylation (**2**) with the low dipole moment values of 3.036 D and 2.862 D have resulted in good antioxidant ability in many real experiments [5, 6]. Polarizability may be justified considering the soluble nature of molecules in polar solvents [21]. Compounds containing sugars and isoflavones **3-4** have generally shown to associate with the higher dipole moment as well as higher polarizability (Table 2). Followed on 4′-methylations and 6-methoxylations, the polarizability is also in accordance with chemical hardness as mentioned above.

Mulliken population analysis (MPA) has resulted in net charges of a chemical ring system which also appears to be an effective tool to assess a chemical reactivity. The Mulliken atomic charges values using the DFT method are presented in Table S2. Generally, the heteroatom oxygens in flavonoids **1–4** remark the significant negative charges, which are active sites of donating their electrons. In the meantime, the maximum of positive charge, which is the preferential site for the nucleophilic reaction has occurred in carbon C-4. The high number of positive (negative) charges of atoms oxygens, carbon, and hydrogen arising from 5-OH and 4-CO is caused by internal hydrogen bonds, thereby stabilizing the structure. The fact is that antioxidant activities of flavonoids further depend on negative centers, whereby hydroxyl groups in ring B are found to act as active sites of radical reactions [20]. As a consequence, considering flavonoid aglycones of studied **3-4** and compound **1**, the high values of negative charges occur in 4′-OH in both gas and methanol, agreeing with the smallest BDE outcome.

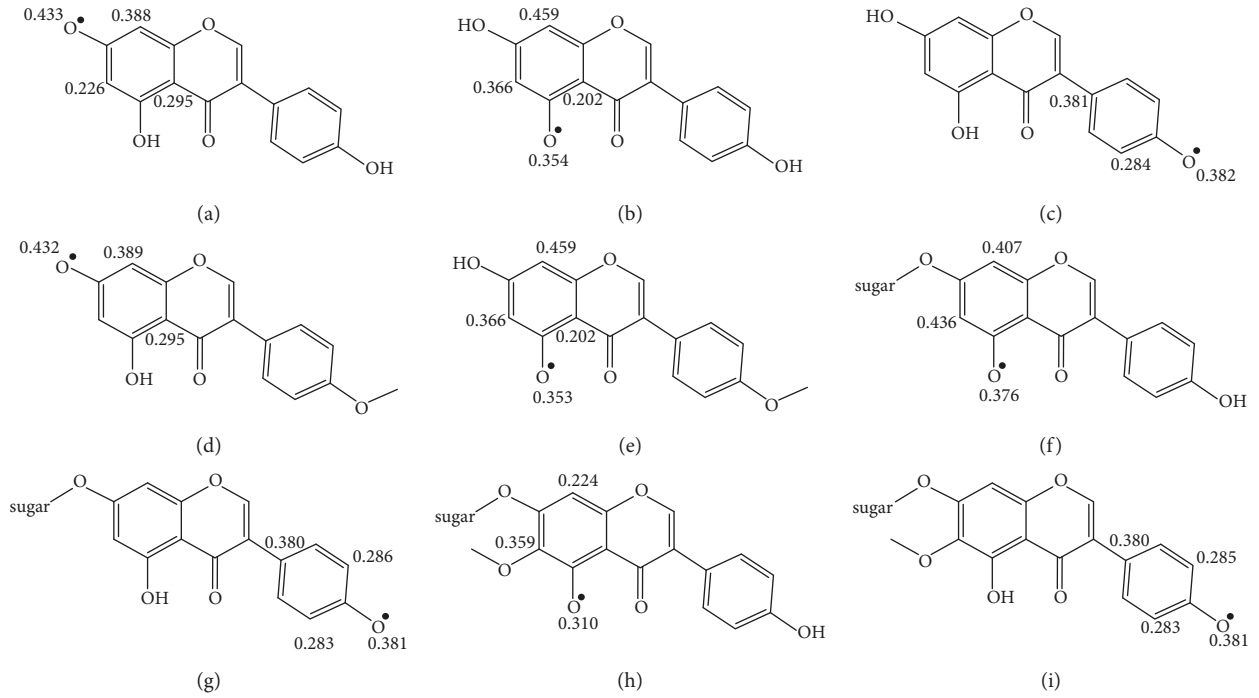

Figure 7: Spin density distribution of structural radicals **1–4** obtained after H-atom abstraction. (a) Compound **1**: 7-OH radical. (b) Compound **1**: 5-OH radical. (c) Compound **1**: 4′-OH radical. (d) Compound **2**: 7-OH radical. (e) Compound **2**: 5-OH radical. (f) Compound **3**: 5-OH radical. (g) Compound **3**: 4′-OH radical. (h) Compound **4**: 5-OH radical. (i) Compound **4**: 4′-OH radical.

Besides frontier molecular orbital considerations and analysis of electronic structure, Fukui parameters also provide important information and quick solutions to justify the powerful reactive site of each atom. Fukui indices from Table S3 are calculated in gaseous medium based on theoretical HSAB principle [31]. It seemed that oxygen of carbonyl group 4-CO of all studied members **1–4** and carbon C-2 in compounds **2** and **4** should have opted as good sites for both electrophilic and radical attacks, but carbon C-2 is the only suitable site of electrophilic scope for metabolites **1** and **3**. 4′-OH in compound **1** and carbon C-6 bears OCH_3 in compound **4**, adapted for nucleophilic attractive types. Most importantly, the f^o condensed Fukui values advocate other preferential radical sites that are found in hydroxyl groups.

Numerous atoms in β-D-apiofuranosyl-(1-6)-β-D-glucopyranosyl parts of compounds **3-4** show the significant Mulliken electronic charges. 4″-OH of glycoside **3** is now expected as electrophilic tendencies, but for further corroboration with HOMO-LUMO analysis above, Fukui descriptors research indicates that sugar units did not show favorability for the antioxidant reactive types, resembling in the computational results in a flavone glycoside rutin or research on pryoanthocyanin [17, 28, 32].

2.4. Antioxidant Mechanisms. In the same condition of 298 K and environmental gas, our BDE results in genistein (**1**), and biochanin A (**2**) differ from the B3LYP/6-31 + G(d,p), and/or B3LYP/6-311++G(d,p) previously calculated publications within usually 4.0 kcal/mol [33, 34]. In addition, our PDE, PA, and ETE numbers show good accordance with B3LYP/6-311++G(d,p) level in the last account performed by Lengyel and partners, particularly the deviation just only found to be 2 kcal/mol in PA calculation, but largely different from the work of Zhang and co-authors [33, 34].

The favorable mechanisms of antiradical activity of isoflavones might possibly be discussed via thermodynamically preferential BDE of HAT, IP of SET-PT, and PA of SPLET actions [35]. From genistein (**1**) in gaseous state reaction in Table 3, BDE values (77.09–94.26 kcal/mol) are significantly lower than those of IP (168.30 kcal/mol) and PA (329.68–347.07 kcal/mol). This behavior is also similarly established from the remainders like **2–4**. Therefore, HAT pathway is probable for isoflavones and isoflavone glycosides in gas.

From a thermodynamic point of view, relating to three well-known mechanisms, the active sites of antioxidant action have also been proposed throughout the minimal sum of enthalpies, including BDEmin in HAT, (IP + PDE) min in SET-PT, and (PA + ETE) min in SPLET [35]. The lowest rank of BDE values ranges from 76.85 to 77.09 kcal/mol is dominated by 4′-OH radical in gas for all isoflavones **1–4**, compared with those of 7-OH radical (83.76–83.84 kcal/mol) and 5-OH radical (85.11–94.26 kcal/mol). A similar instance arises from enthalpies of SET-PT and SPLET pathways that either isoflavones **1-2** or their glycosides **3-4** also encompasses the minimum values of IP + PDE and PA + ETE at 4′-OH. Once again, it can be seen that ring B of isoflavones and 4′-OH are active centers involving in antioxidant activity. Although electron transfer enthalpy (ETE) shows the lowest amount in all radical cases of **1–4**, minimal

Table 3: Gas phase reaction enthalpies at 298 K for radicals of the studied compounds at B3LYP/6-311G(d) level of theory (in kcal/mol).

Compounds	HAT BDE	IP	PDE	SET-PT (IP + PDE)	PA	ETE	SPLET (PA + ETE)
1		168.30					
5-OH	94.26		241.66	409.96	347.07	62.89	409.96
7-OH	83.84		231.36	399.66	329.68	70.02	399.70
4′-OH	77.09		224.49	392.79	337.90	55.89	393.79
2		165.79					
5-OH	94.26		244.19	409.98	347.40	62.57	409.97
7-OH	83.76		233.68	399.47	330.00	69.62	399.62
3		164.76					
5-OH	94.14		245.09	409.85	348.02	61.83	409.85
4′-OH	76.89		227.84	392.60	338.11	54.49	392.60
4		157.17					
5-OH	85.11		243.72	400.89	345.63	55.19	400.82
4′-OH	76.85		235.42	392.69	338.22	54.29	392.51

total energies of PA + ETE and IP + PDE establish 4 times more potency than those of BDE. This is sequential evidence to deeply vindicate that HAT mechanism gets more favor in gas. Here, we can make an arrangement in the following order of favorable: HAT > SET-PT ≈ SPLET, and importantly conclude that in the environmental gas and antioxidant mechanisms have been becoming dependent on the processes of proton disruptions rather than the effects of electron actions.

In terms of comparing among radicals 5-OH, 7-OH, and 4′-OH in each metabolite, O-H homolytic bond dissociation enthalpy (BDE), O-H heterolytic bond dissociation enthalpy (PDE), and proton affinity (PA) are realistic evidence would since have been proved that energies of 5-OH bond breaking always overcome due to IHBs (Table 3).

Antioxidant-structural relationships can be highlighted through the differences in enthalpies calculations. When spontaneously compared two isoflavone glycosides **3-4**, 5-OH radical enthalpy parameters BDE, IP, PDE, PA, and ETE, the courses of IP + PDE and PA + ETE of compound **4** are less than those of 5-OH radical in compound **3** from 2 to 9 kcal/mol. It therefore remarks that 6-OCH_3 has greatly influenced 5-OH and IHBs, so that the 6-methoxylation would help increase antioxidant. In the same assessment for compounds **1-2**, 4′-methylation did not significantly contribute to the effect itself on 5-OH and 7-OH radicals, but the reverse trends are observed: 5-OH radical BDE in genstein (**1**) > biochanin A (**2**), 5-OH and 7-OH radicals PDE in genistein (**1**) < biochanin A (**2**). As mentioned above, *β*-D-apiofuranosyl-(1-6)-*β*-D-glucopyranosyl unit should not be the suitable sites for radical scavenging but they have greatly affected isoflavone core. Indeed, 7-glycosylation (*meta* position) in ambocin (**3**) has two sides. On the one hand, it shows a decrease in the amount of energy in 5-OH bond breaking in terms of BDE, IP, IP + PDE, ETE, and PA + ETE, while on the other hand, it induces an increase pattern in those in PDE and PA, as compared with 7-hydroxylation in genistein (**1**).

Last but not least, among **1** and **3-4**, 4′-OH radical BDE leads to the introduction of an actively antioxidant arrangement: tectorigenin 7-*O*-[*β*-D-apiofuranosyl-(1-6)-*β*-D-glucopyranoside] (**4**) > ambocin (**3**) > genistein (**1**), while no change is observed in 7-OH radical BDE values and 5-OH radical one with the order genistein (**1**) < biochanin A (**2**).

3. Conclusion

Naturally occurring isoflavones and their glycosides have successfully been investigated by the density theory-based method. Actually, the prospective outcome points out that HAT pathway is preferentially closely related to the antioxidant action of all studied polyphenolic compounds in the gaseous state. Numerous parameters, such as ionization potential (IP), proton affinity (PA), the sum of energies of SET-PT, and/or SPLET mechanisms, especially in terms of BDE values, provide supportive information to confirm the radical-scavenging process that takes place throughout O-H breaking bond in isoflavones. This current result corresponds to many previous studies, in which structural conformations, *π*-electrons delocalization, potential polarizability, hydroxyl groups distributed in ring B, and functional groups are major reasons for antioxidant activities of general flavonoids. Antioxidant isoflavone glycosides ambocin and tectorigenin 7-*O*-[*β*-D-apiofuranosyl-(1-6)-*β*-D-glucopyranoside] are more significant than isoflavone genistein and biochanin A deducing from 7-glycosylation and 6-methoxylation. This account provides necessary guidelines for future research.

Abbreviations

DFT: Density functional theory
HOMO: Highest occupied molecular orbital
LUMO: Lowest unoccupied molecular orbital
IHBs: Intramolecular hydrogen bonds
BDE: Homolytic bond dissociation enthalpy
PDE: Heterolytic bond dissociation enthalpy
IP: Ionization potential
PA: Proton affinity
ETE: Electron transfer enthalpy
HAT: Hydrogen atom transfer
SET-PT: Single electron transfer-proton transfer
SPLET: Sequential proton loss electron transfer
DPPH: 2,2-Diphenyl-1-picrylhydrazyl.

Data Availability

All data used for this project are publicly available and accessible online. The authors have pronounced the entire data building process and empirical techniques presented in the paper.

Conflicts of Interest

The authors declare that they have no conflicts of interest.

Acknowledgments

This work was supported by a grant (no. VAST.CTG.01/17-19) from Vietnam Academy of Science and Technology (VAST), 18 Hoang Quoc Viet, Caugiay, Hanoi, Vietnam.

Supplementary Materials

Figure S1: the state forms of studied structures in MeOH medium. Table S1: the collective energies depended on torsional angles θ_2 (C2-C3-C1′-C2′). Table S2: Mulliken atomic charges at theoretical level B3LYP/6-311G(d) of studied compounds in gas and methanol mediums. Table S3: condensed Fukui indices at B3LYP/6-311G(d) of studied compounds in gas medium. (*Supplementary Materials*)

References

[1] E. Miadoková, "Isoflavonoids-an overview of their biological activities and potential health benefits," *Interdisciplinary Toxicology*, vol. 2, no. 4, pp. 211–218, 2009.

[2] A. N. Panche, A. D. Diwan, and S. R. Chandra, "Flavonoids: an overview," *Journal of Nutritional Science*, vol. 5, p. e47, 2016.

[3] Z. Dhaouadi, M. Nsangou, N. Garrab, E. H. Anouar, K. Marakchi, and S. Lahmar, "DFT study of the reaction of quercetin with and radicals," *Journal of Molecular Structure: THEOCHEM*, vol. 904, no. 1-3, pp. 35–42, 2009.

[4] P. Dixit, R. Chillara, V. Khedgikar et al., "Constituents of Dalbergia sissoo Roxb. leaves with osteogenic activity," *Bioorganic & Medicinal Chemistry Letters*, vol. 22, no. 2, pp. 890–897, 2012.

[5] J. N. Choi, K. Dockyu, K. C. Hyung, M. Y. Kyung, K. Jiyoung, and H. L. Choong, "2′-Hydroxyaltion of genistein enhanced antioxidant and antiproliferative activities in MCF-7 human breast cancer cells," *Journal of Microbiology and Biotechnology*, vol. 19, pp. 1348–1354, 2009.

[6] S. Dowling, F. Regan, and H. Hughes, "The characterisation of structural and antioxidant properties of isoflavone metal chelates," *Journal of Inorganic Biochemistry*, vol. 104, no. 10, pp. 1091–1098, 2010.

[7] J.-G. Cho, H.-J. Park, G.-W. Huh et al., "Flavonoids from Pueraria mirifica roots and quantitative analysis using HPLC," *Food Science and Biotechnology*, vol. 23, no. 6, pp. 1815–1820, 2014.

[8] Y. Zhang and Y. Sun, "Theoretical investigation on atmospheric reaction of O(3P) with CH 2 CN," *Journal of Physical Organic Chemistry*, vol. 32, no. 4, article e3913, 2018.

[9] E. M. Kamel, A. M. Mahmoud, S. A. Ahmed, and A. M. Lamsabhi, "A phytochemical and computational study on flavonoids isolated from *Trifolium resupinatum* L. and their novel hepatoprotective activity," *Food & Function*, vol. 7, no. 4, pp. 2094–2106, 2016.

[10] R. A. Mendes, S. K. C. Almeida, I. N. Soares et al., "A computational investigation on the antioxidant potential of myricetin 3,4′-di-O-α-L-rhamnopyranoside," *Journal of Molecular Modeling*, vol. 24, no. 6, p. 133, 2018.

[11] K. S. Kumar and R. Kumarresan, "A DFT study on the structural, electronic properties and radical scavenging mechanisms of calycosin, glycitein, pratensein and prunetin," *Computational and Theoretical Chemistry*, vol. 985, pp. 14–22, 2012.

[12] A. Vaganek, J. Rimarcik, V. Lukes, L. Rottmannova, and E. Klein, "DFT/B3LYP study of the enthalpies of Homolytic and Heterolytic O-H Bond dissociation in sterically hindered phenols," *Acta Chimica Slovenica*, vol. 4, pp. 55–71, 2011.

[13] M. Leopoldini, T. Marino, N. Russo, and M. Toscano, "Antioxidant properties of phenolic compounds: H-atom versus electron transfer mechanism," *Journal of Physical Chemistry A*, vol. 108, no. 22, pp. 4916–4922, 2004.

[14] R. A. Mendes, B. L. S. Silva, R. Takeara, R. G. Freitas, A. Brown, and G. L. C. de Souza, "Probing the antioxidant potential of phloretin and phlorizin through a computational investigation," *Journal of Molecular Modeling*, vol. 24, no. 4, p. 101, 2018.

[15] E. N. Maciel, S. K. C. Almeida, S. C. da Silva, and G. L. C. de Souza, "Examining the reaction between antioxidant compounds and 2,2-diphenyl-1-picrylhydrazyl (DPPH) through a computational investigation," *Journal of Molecular Modeling*, vol. 24, no. 8, p. 218, 2018.

[16] A. Galano, G. Mazzone, R. A. Diduk, T. Marino, J. R. A. Idaboy, and N. Russo, "Food antioxidants: chemical Insights at the Molecular Level," *Annual Review of Food Science and Technology*, vol. 7, no. 1, pp. 335–352, 2016.

[17] V. B. Luzhkov, "Mechanisms of antioxidant activity: the DFT study of hydrogen abstraction from phenol and toluene by the hydroperoxyl radical," *Chemical Physics*, vol. 314, no. 1-3, pp. 211–217, 2005.

[18] S. A. P. Gomez, N. F. Holguin, A. P. Hernandez, M. P. Miramontes, and D. G. Mitnik, "Computational molecular characterization of the flavonoid rutin," *Chemistry Central Journal*, vol. 4, no. 1, p. 12, 2010.

[19] D. G. Mitnik, "Computational chemistry of natural products: a comparison of the chemical reactivity of isonaringin calculated with the M06 family of density functionals," *Journal of Molecular Modeling*, vol. 20, no. 7, p. 2316, 2014.

[20] H. Djeradi, A. Rahmouni, and A. Cheriti, "Antioxidant activity of flavonoids: a QSAR modeling using Fukui indices descriptors," *Journal of Molecular Modeling*, vol. 20, no. 10, p. 2476, 2014.

[21] K. Sadasivam and R. Kumaresan, "Antioxidant behavior of mearnsetin and myricetin flavonoid compounds-a DFT study," *Spectrochimica Acta Part A: Molecular and Biomolecular Spectroscopy*, vol. 79, no. 1, pp. 282–293, 2011.

[22] R.-M. Han, Y.-X. Tian, Y. Liu et al., "Comparison of flavonoids and isoflavonoids as antioxidants," *Journal of Agricultural and Food Chemistry*, vol. 57, no. 9, pp. 3780–3785, 2009.

[23] S. F. Farag, A. S. Ahmed, K. Terashima, Y. Takaya, and M. Niwa, "Isoflavonoid glycosides from *Dalbergia sissoo*," *Phytochemistry*, vol. 57, pp. 1263–1268, 2001.

[24] S. T. Ninh, "A Review on the medicinal plant Dalbergia odorifera species: phytochemistry and biological activity," *Evidence-Based Complementary and Alternative Medicine*, vol. 2017, Article ID 7142370, 27 pages, 2017.

[25] A. Kuzniar, J. Pusz, and U. Maciolek, "Potentiometric study of Pd(II) complexes of some flavonoids in water-methanol-1,4-dioxane-acetonitrile (MDM) mixture," *Acta Poloniae Pharmaceutica*, vol. 74, pp. 369–377, 2017.

[26] K. Benthami, S. A. Lyazidi, M. Haddad, M. Choukrad, B. Bennetau, and S. Shinkaruk, *Photophysics of Genistein and Biochanin A Isoflavones: Solvent Cage and Concentration Effects Studied by UV Visible Spectroscopy*, Nova Science Publishers, Inc., Hauppauge, NY, USA, 2009, ISBN: 978-1-61728-113-6.

[27] P. Trouillas, P. Marsal, D. Siri, R. Lazzaroni, and J.-L. Duroux, "A DFT study of the reactivity of OH groups in quercetin and taxifolin antioxidants: the specificity of the 3-OH site," *Food Chemistry*, vol. 97, no. 4, pp. 679–688, 2006.

[28] M. Ghiasi and M. M. Heravi, "Quantum mechanical study of antioxidative ability and antioxidative mechanism of rutin (vitamin P) in solution," *Carbohydrate Research*, vol. 346, no. 6, pp. 739–744, 2011.

[29] L. H. M. Heravi, C. H. Rios-Reyes, N. J. Olvera-Maturano, J. Robles, and J. A. Rodrigues, "Chemical reactivity of quinclorac employing the HSAB local principle-Fukui function," *Open Chemistry*, vol. 13, no. 1, p. 52, 2015.

[30] K. Sadasivam and R. Kumaresan, "A comparative DFT study on the antioxidant activity of apigenin and scutellarein flavonoid compounds," *Molecular Physics*, vol. 109, no. 6, pp. 839–852, 2011.

[31] K. O. Sulaiman and A. T. Onawole, "Quantum chemical evaluation of the corrosion inhibition of novel aromatic hydrazide derivatives on mild steel in hydrochloric acid," *Computational and Theoretical Chemistry*, vol. 1093, pp. 73–80, 2016.

[32] M. Leopoldini, F. Rondinelli, N. Russo, and M. Toscano, "Pyranoanthocyanins: a theoretical investigation on their antioxidant activity," *Journal of Agricultural and Food Chemistry*, vol. 58, no. 15, pp. 8862–8871, 2010.

[33] J. Lengyel, J. Rimarčík, A. Vagánek, and E. Klein, "On the radical scavenging activity of isoflavones: thermodynamics of O-H bond cleavage," *Physical Chemistry Chemical Physics*, vol. 15, no. 26, p. 10895, 2013.

[34] J. Zhang, F. Du, B. Peng, R. Lu, H. Gao, and Z. Zhou, "Structure, electronic properties, and radical scavenging mechanisms of daidzein, genistein, formononetin, and biochanin A: a density functional study," *Journal of Molecular Structure: THEOCHEM*, vol. 955, no. 1-3, pp. 1–6, 2010.

[35] D. Amic, V. Stepanic, B. Lucic, Z. Markovic, and J. M. D. Markovic, "PM6 study of free radical scavenging mechanisms of flavonoids: why does O–H bond dissociation enthalpy effectively represent free radical scavenging activity?," *Journal of Molecular Modeling*, vol. 19, no. 6, pp. 2593–2603, 2013.